Microsystem Technologies 5 (1999) 173–180 © Springer-Verlag 1999

Control tribological and mechanical properties of MEMS surfaces. Part 1: critical review

Z. Rymuza

Abstract The problem of modification of rubbing surfaces in micrometer size microdevices (micro-electro-mechanical systems – MEMS) to control adhesion, friction and wear as well as mechanical properties is discussed. Several solutions are reviewed and examples of investigation results are given.

Introduction

Microelectromechanical systems (MEMS) are extremely miniaturized devices which are in recent years produced for a wide range of electronic applications. Such microscale movable mechanical elements as pin joints, gears, springs, cranks, sliders, turbines, etc., are manufactured using, in particular, Integrated Circuits (IC) – compatible microfabrication processes [1]. Micromechanical sensors and electric micromotors are also produced using mainly silicon as the base material.

Surface microstructures are now manufactured using three different micromachining processes: surface micromachining, bulk micromachining, and the LIGA process. In these methods photolithography, material deposition, etching and electroplating are used to fabricate the microstructures.

When MEMS, in particular are surface micromachined, they often embody microelements with smooth and chemically active surfaces. Interactions between the MEMS surfaces is critical to the behaviour of such systems since the kinetic energies , start-up forces and torques in their operation, and hence available to overcome retarding forces, are necessarily small [2].

Surface effects are extremely important in every unintentional and normal contact during operation. Topography, mechanical properties and tribological behaviour of MEMS interfaces play a paramount role in the reliability and robustness of such devices. Control of the state of contacting (rubbing) surfaces of microstructures is the effective means of enhancing the reliability and performance of microsystems.

Received: 30 June 1998/Accepted: 14 December 1998

Z. Rymuza
Institute of Micromechanics and Photonics, Department of Mechatronics, Warsaw University of Technology, ul.Chodkiewicza 8, 02-525 Warszawa, Poland

Correspondence to: Z. Rymuza

Fabrication, design, ambient and performance of MEMS

The reliability and lifetime of MEMS are very dependent on fabrication, design and operational environment. The fabrication process has an impact on the performance characteristics of a microsystem through the reproduction accuracy of the design geometry and through the modification of the characteristics of the contacting surfaces. Fabrication has a significant impact on the microsystem geometrical design through pattern definition. Through deposition and/or etching, fabrication affects the characteristics of the surfaces which will be in mechanical contact in MEMS. The performance of the system is also indirectly affected by the mechanical properties of the structural material, e.g. residual stress induced deformations in the structural material may limit the range of rotor radius (in a micromotor) and thickness that can be successfully fabricated thereby affecting the micromotor motive torque.

Fabrication plays an important role in defining the characteristics of the surfaces which will be in frictional contact during MEMS operation. The frictional characteristics of the mechanical contact is influenced by the texture of the contacting surfaces. The bearing surface is comparatively smooth if it is created by an isotropic wet chemical etch but at delineation by reactive ion etching (RIE) of polysilicon the etched side walls of the pattern are rough on a microscopic scale. The roughness gives rise to significant intitial wear out [3,4]. On the air gap side walls in a micromotor, this roughness can lead to localized electric field concentration and therefore premature breakdown.

A notorious problem of surface micromachined structures using the sacrificial layer etching technique is the permanent attachment of slender structures to the underlying substrate after drying. The stiction (permanent adhesion) during post-etch rinsing is initiated by high surface tension forces resulting from trapped rinse liquid in the capillary-like spaces between the microstructures and the substrate [4–7]. The magnitude of these capillary forces is in some cases sufficient to deform and pin the structures to the substrate resulting in device failure.

Stiction can be prevented or reduced in several ways which can roughly be divided into two groups [6,7]. First, there are methods based upon the prevention of physical contact between structures and the substrate during fabrication (e.g. by using dry etching techniques), second there are methods based upon the reduction of adhesional forces (by minimizing the surface free energy, reduction of the real area of contact etc.). Also, elevated temperature solvent rinses are shown to be further decreased by drying at high temperature in a rapid

thermal annealer which suggests that instability of the trapped liquid under tension at elevated tepmeratures may be a dominant factor in reducing stiction.

Microsystem release and testing is a determining step for its successful operation [8–12]. Release and testing procedures can affect the frictional characteristics of microsystems significantly. The studies of early side-drive micromotors, which did not include a shield under the rotor, indicated that substrate clamping of the rotor inhibited micromotor operation [13]. The clamping force was attributed to an electric field between the rotor and the silicon substrate. One of the ways to overcome this clamping, resulted in excessive friction, is use of an electric shield, positioned under the rotor and in electrical contact with it [14]. A dry nitrogen source was used to levitate the rotor to compensate for the clamping force [13]. However, even with incorporated electric shields, nitrogen levitation is sometimes necessary to overcome frictional forces associated with the clamping of the rotor to the shield because the lack of proper electrical contact between the rotor, the shield, and the bearing.

Even though the rotor clamping mechanism described above plays a critical role in micromotor operation, other effects are also significant. The release process and operational environment may modify the magnitude of the coefficient of friction of the contact surfaces by changing the surface characteristics, thereby modifying the frictional torque magnitude.

Another important factor is contamination of the surfaces being a function of the release processes. The presence of contaminants that may have been left behind on the rotor/bearing and shield/bearing contact surfaces due to release process could contribute to the increase of friction [8].

The design of a microsystem is important. Drive systems, in particular, rotating electrostatic micromotors are fabricated by surface micromachining using polysilicon with a thickness of only a few micrometers [1, 8]. The driving torque is rather small and, in addition, lifetime is limited due to friction. Micromotors with large heights can be fabricated by the LIGA process or an integrated multilayer high aspect ratio process or other non-traditional technologies [1, 11, 15, 16]. LIGA structures can be made from metal or polymer or even ceramics and are typically a few hundred micrometers high.

In the field of electrostatic micromotors there are three different types: the variable capacitance, the electroquasi-induction micromotors and harmonic (wobble) micromotors. In wobble micromotors the reduction of friction caused by the rotor on the axle is obtained by a rolling motion [1, 3, 8, 15]. The central feature of the wobble micromotor is that the rotor wobbles around the centre bearing post. Two types of bearings are used in micromotors: centre-pin and flange bearings (Fig. 1).

Flange bearing wobble micromotors show superior performance in gaseous environments over their centre-pin counterparts [17]. They can be operated in room air for longer periods and are not significantly affected by the operating environment or by extended storage between operations. These improvements result from the fact that the flange has a smaller lever arm than the bushing resulting in a smaller friction torque.

Bearing backsides of a micromotor are made usually with three hemispherical bushings. In order to further reduce of bushing friction a unique needle-shaped bushing was proposed [16]. The needle-shaped bushing has lower friction compared with the traditional solution (Fig. 1b) since the load is smaller for this kind of the bearing structure. Two major sources of the load are electrostatic forces and capillary force. A little wear on the tip of needle bushing after 3.6 millions of revolutions was revealed [16].

The application of a special gas-lubricated bearing was also proposed [18, 19]. An aerodynamic in-pumping spiral grooved thrust microbearing with a groove width of four micrometers and a groove depth of 300 nm has been designed and used in micromotors.

The prismatic shape of the bearings is more effective for reduction of friction and wear as compared to the traditional cylindrical shaped bearings [20, 21]. This is because of the transfer of wear debris into the corners of a prism.

The reason why friction causes trouble with MEMS is that the friction force obeys an unfavourable scaling law in microdomains. When the characteristic dimension L is decreased, the frictional force decreases in proportion to the square of L and the inertial force in proportion to cubic L. Therefore, the frictional force dominates over inertial force in small dimensions and prevents, e.g. rotors or microgears from moving smoothly. The smaller the elements are, the higher the friction that should be expected.

There are three micromotor parameters that affect the final device operational characteristics: the motor air-gap size, bearing radius and bearing clearance [1, 8, 15]. Holding all other MEMS parameters constant, reducing the air-gap size increases the motive torque. Increasing the bearing radius increases the bearing frictional force. This is of particular importance for the salient-pole micromotors in which the bearing operation results in sliding contacts [8, 13, 14, 22].

For a centre-pin-bearing salient-pole micromotor, performance is optimized by minimizing the bushing and the bearing radii. The bushing frictional torque is proportional to the bushing radius (i.e. bushing distance from the micromotor centre). For the wobble micromotors (Fig. 2 [15, 23]) in which ratio (for definition see caption to Fig. 2) and motive torque are proportional to the bearing radius. In this case, increasing the bearing radius leads to enhanced motive torque (with

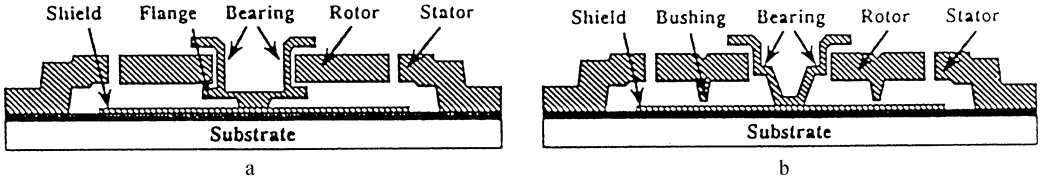

Fig. 1. Cross-sectional schematic of flange **a** and center-pin **b** bearings of a micromtor

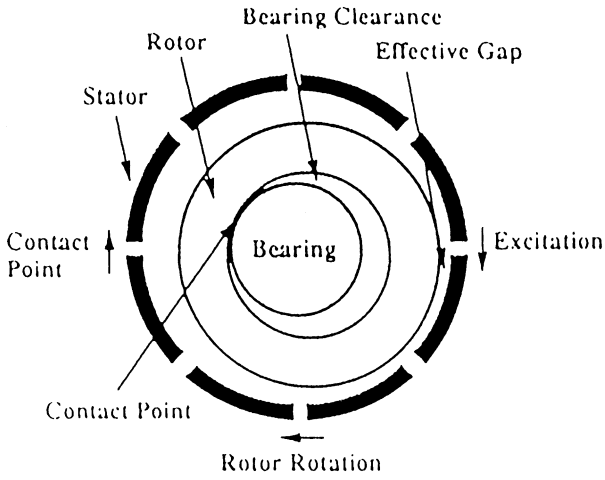

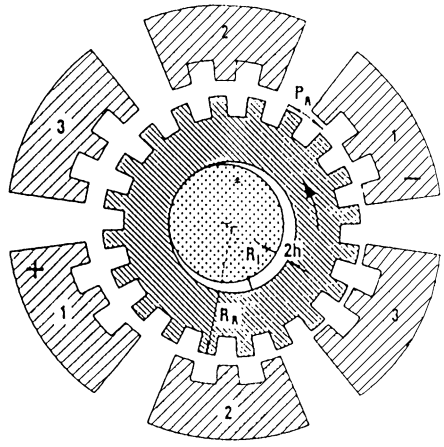

Fig. 2. Schematic plan views of a typical wobble micromotor **a** and a wobble stepping micromotor driven by three-phase voltage **b**. Gear ratio of a wobble motor is ratio of electrical excitation frequency to rotor rotational frequency, i.e. ratio of radius of bearing and bearing clearance

increasing bearing radius) which is expected to be larger than the increase in the bushing friction torque, resulting in an increase in the micrometer net output torque.

During wobble micromotor operation, the rotor is pulled against the bearing due to the normal electric force and rolls on the bearing so the resulting friction at the bearing contact is critical to the micromotor operation. However, for the salient-pole micromotors, bearing frictional forces are detrimental to micromotor performance [8, 13, 22, 24, 25].

During motion the contact point in a wobble micromotor travels around the axle and causes considerable friction. Since the radial force, experienced by the rotor resulting from an unstable electrostatic equilibrium between the two active stators, is larger than the tangential driving force, the coefficient of friction has to be as small as possible. Otherwise, motion might be prevented or lifetime reduced dramaticallly. The rotor should roll on the axle instead of sliding on it. The rotor slip (because of sliding) affects, in practice, the gear ratio which is the function of motive and friction torques [3, 23]. Because of sliding, the gear ratio is somewhat larger than ideal or nominal gear ratio (which is equal to the bearing radius divided by the bearing clearance). The gear ratio is also affffected by wear in the bearing, which results in an increase in the bearing clearance [3]. The rotor slip should be minimized since it does not produce output torque but dissipates motive torque.

Since the bearing operation in the wobble micromotors produces rolling contacts, the bearing frictional torque is small and is further offset by the dependence of motive torque on the bearing radius. Due to the bearing anchor pattern definition and delineation requirements, the bearing radius cannot be reduced arbitrarily [8–10]. Increasing the bearing radius leads to enhanced motive torque through an increase of the gear ratio, however, the bushings would then have to be located further through an increase of the gear ratio, however, the bushings would then have to be located further out from the micromotor centre, leading to increased bushing friction torque.

As it was mentioned above, the third important parameter affecting the final device operational characteristics is bearing clearance. In general, both salient-pole and wobble micromotor performance is enhanced by minimizing the bearing clearance [3, 8–10, 15, 22]. For the salient-pole micromotors, smaller bearing clearances result in reduced side pull and therefore reduced bearing friction. For the wobble micromotor, smaller bearing clearances result in increased gear ratio and therefore increased motive torque. The smallest bearing clearance reported for polysilicon micromotors is 300 nm [8–10, 22]. It is believed that an eventual bearing clearance of 100 nm with improvements in rotor/stator pattern definition and delineation is possible [9]. For micromotors made by the LIGA process if the structural height exceeds 0.1 mm the bearing clearance can be hardly smaller than 250 nm [15, 20]. It is important to have very small bearing clearances in such micromotors. The realization of smaller (than 250 nm) bearing clearances requires to use assembling techniques [26], which lower the integration level of the fabrication sequence.

Polysilicon surface roughness significantly affects micromotor fabrication by limiting pattern definition and delineation [1, 8–10, 12]. First , the micromotor operation is controlled by the rotor/stator gap size which is adversely affected by polysilicon roughness. Second, the resist pattern edges develop asperities as the resist is patterned over a rough polysilicon surface [1, 8–10, 12]. The former limits the motive torque and the latter leads to interlocking asperities between the rotor inner radius and the bearing outer radius. The rotor inside radius has not a perfect circular shape but has small sharp asperities superimposed on its circular shape. The bearing clearance size is also related to the size of the rotor inner radius asperities and must be increased appropriately for increasing rotor inner radius side wall roughness. The interlocking asperities in the bearing still disrupt smooth micromotor operation even when the bearing clearance is large [1, 8, 9, 21, 22].

The roughness on the rotor inner radius side wall gives rise to significant initial wear in the micromotor bearing as the side

wall asperities wear out [1, 3, 4, 8, 22]. The polysilicon shield surface is characteristically rough on the microscopic scale but the bushing surface which slides on the shield is comparatively smooth. The roughness of the shield surface reduces the real area of contact between the bushing and the shield significantly and the real area of contact is comparatively small in all cases (at various bushing-shield apparent area of contact). The roughness of the rougher surfaces in polysilicon micromotors is of the order of 60 nm [1, 3, 8, 9]. To reduce polysilicon surface roughness it is necessary to reduce the oxidation (thermal oxide is used as the polysilicon etch mask) temperature (the roughness increases with the logarithm of the oxidation temperature [9]).

Materials are important to reduce friction and wear and therefore to improve reliability and to extend lifetime. Polysilicon is the most commonly used material in micromachining because the process is well established, it has good mechanical properties and the integration with electronics and sensors is possible [1, 8, 22, 27, 28]. Other materials such as polyimide, tungsten, nickel, copper, gold are used as structural materials [1, 9–12, 27]. To reduce friction and wear thin films of, e.g. silicon nitride, diamond-like carbon (DLC) are also applied [1, 14, 16, 22, 24, 29]. The ion-implanted silicon demonstrates bettter tribological behaviour than unimplanted silicon [30, 31].

Friction and wear in sliding contacts in MEMS depend significantly on the materials involved in sliding. The fabrication of MEMS such as micromotors is mainly based on silicon and its compounds and their tribological behaviour plays a key role in the performance of such systems. From friction and wear studies of various combinations of materials applicable in microsystems it is observed that DLC sliding on DLC shows low friction and low wear rate [4, 8, 17, 28, 29, 32–38]. The static friction coefficient of silicon can vary from very low values when rubbing against silicon oxide (below 0.1) to relatively high values in silicon–molybdenum systems (0.45) [34].

Ambient (atmosphere, humidity, presence of fluid/lubricant, temperature, etc.) plays an important role in the tribological behaviour of MEMS. The effect of the environment depends on the design of the bearings. As it was aforementioned, the smaller lever arm in comparison with the bushing results in a flange bearing wobble micromotor with generally better performance in gaseous environments as compared to their centre-pin bearing counterparts [8, 9, 17]. They can operate in room air for longer periods and are not significantly affected by the operating environment or by extended storage between operations. The results from a comparative study of the operation of flange and centre-pin bearings show that for centre-pin bearings the coefficient of friction for polysilicon on polysilicon is 0.38 for operation in nitrogen and argon atmosphere, 0.48 for operation in oxygen and 0.54 for operation in room air [17]. A small increase in the flange/bushing normal contact force was increased in room air as compared to nitrogen. The coefficient of static friction of silicon nitride on silicon nitride, silicon nitride on single-crystal silicon, silicon dioxide on single-crystal silicon in the presence of oxygen are higher than that in the presence of argon and nitrogen [32]. Nitrogen acts as a lubricant, and adsorbed oxygen acts as an adhesive between the silicon and silicon compounds. The oxide formation and growth are important factors in the sliding wear of silicon and, in general, they tend to increase wear [39].

In ultrahigh vacuum the coefficient of static friction between silicon and the aforementioned silicon compounds is in the range 0.2–0.7 [32].The DLC–DLC sliding contact exhibits the coefficient of friction only 0.04 in the same UHV [32]. Oxygen exposure increases the coefficient of friction by 50% between DLC–DLC, but this value is still an order of magnitude smaller than that between silicon-based materials.

Effect of humidity (moisture) is such that, e.g. the coefficients of friction between silicon dioxide–silicon dioxide and silicon dioxide–silicon contacts increase by 55–157% with increased exposure to humidity [32]. A similar effect was also observed for DLC-DLC sliding contacts [29]. The adsorption of water molecules can cause stiction to stop a microsystem from functioning. The increase in frictional resistance due to stiction depends largely on the structure of water molecules. It was found that the water molecules situated near the surface, e.g. three or four layers of water, behave like pseudo-solid and that they were highly viscous [40]. The tribochemical reactions occur during wear of silicon surfaces in the presence of oxygen and water vapour [41]. The Si–H bonding are extensively formed in wear particles of silicon in a humid atmosphere. The OH concentration in wear particles increases with humidity.

Many future medical, as well as some industrial applications of microsystems would require device operation in a liquid environment. Surface-micromachined polysilicon microengines and wobble-side-drive electrostatic micromotors with flange and centre-pin bearing designs were successfully operating in DI water and silicone lubricating oils [12, 42, 43]. The micromotor operation in liquids was found to be dominated by viscous drag [42, 43]. Viscous air or fluid damping occur in laterally driven (oscillating) planar microstructures (microresonators). In these lateral microdevices (resonant sensors and actuators, microfilters, damped microaccelerometers) fluid films ambient to the microstructures behave as linear slide-film dampers. As the ratio of surface area to fluid thickness increases in the surface micromachined structures, viscous damping in the ambient fluid increases rapidly, becoming the major source of energy dissipation [44–46].

At high-temperature silicon shows a large adhesive force so a movement of MEMS would get worse with increase of temperature. The static friction coefficient of silicon wafer against silicon wafer increases with increase of temperature (from 0.5 at 20°C to about 0.8 at 200°C) [47]. This is caused by increase of the adhesive force between silicon wafers. However, the frictional force does not vary as a function of temperature when a silicon wafer is coated with silicon dioxide or aluminium thin (over 100 nm) films. In very small micromotors the heat generation due to viscous drag in air gap between the rotor and the silicon substrate and in frictional contacts can be enough intensive [48, 49].

Load and sliding speed are important parameters influencing tribological behaviour of a system. The friction and wear of silicon on sliding on diamond is a function of load [50]. The friction coefficient for silicon sliding on various materials, in general, decreases at increase of load [28]. The effect of contact

pressure, as investigated for polysilicon microstructures [35, 37, 38] was largely as from macroscopic theory although the increase in wear rates with contact pressure was not linear.

Lubrication and modification of MEMS surfaces

Lubrication by gas when sliding surfaces are covered by an adsorbed monolayer of a gas is effective but at higher loads in order to lubricate, e.g. a micromotor of micrometer size, the only way to use real lubricants is to build ultrathin layers with these products, on the rubbing surfaces, preferably long-chain molecules because of their well-known ability for the lubrication of contacts on the macroscopic scale. There are three ways to obtain well organized and dense layers: the Langmuir–Blodgett method, chemical adsorption at room temperature and chemical grafting of molecules.

Traditional lubrication involves the use of multimolecular layers of organic substances that can physically or chemically adsorb onto polar surfaces by their functional groups to form close-packed arrangements of lubricant chains oriented almost perpendicularly to the substrate surface. In the case of MEMS, lubricant selection is complicated. For example, the high-temperatures encountered during fabrication preclude the use of lubricants before the final release-etch processing step. Fluid lubricants, as it was aforementioned, may introduce capillary and viscous shear mechanisms which will result in energy dissipation. The ideal lubricants for MEMS are ultrathin layers covalently bonded to microelement surfaces.

Grafting of densely packed organic molecules on microstructure surfaces to obtain nanometer-thick monolayers is the best way because typical surface separation distances are in the range 500–2000 nm. Such monolayers must exhibit high hydrophobicity and low surface energies to minimize effect of capillary forces, low friction to yield minimal energy losses, and high wear resistance and stability within a wide range of environmental conditions for reliable operation over long-time periods. Their application should be compatible with the wet release process.

The formation of these well-organized organic monolayers occurs spontaneously upon the exposure of a suitable surface to a solution of assembling molecules possessing reactive functionalities, they are often referred to as self-assembled monolayers (SAM). There are various types of SAM coatings. Long-chain hydrocarbon and fluorocarbon molecules are good candidate lubricants for MEMS because they can form chemically bound and highly ordered monolayers on hydroxyl-terminated surfaces such as those of oxidized polysilicon, silicon nitride, aluminium, etc. [2, 51–54, 67, 68, 72].

One of the interesting compounds useful for MEMS lubrication is n-octadecyltrichlorosilane (OTS), n-$C_{18}H_{37}SiC_{13}$ which gives complete coverage of smooth surfaces of n-type silicon by densely packed monolayers formed by chemisorption of silane compounds incorporated in solutions [55]. Sliding experiments with glass spheres and p-type smooth silicon wafers coated with n-$C_{18}H_{37}SiC_{13}$, n-$C_{11}H_{23}SiC_{13}$ (UTS), and n-$C_6F_{13}CH_2CH_2SiC_{13}$ (FTS) [55] have shown insignificant wear and relatively low friction for OTS and UTS monolayers (friction coefficients 0.07 and 0.09, respectively), and significantly higher friction (friction coefficient 0.16) and wear for FTS monolayers, presumably due to incomplete coverage of silicon surface by the thinner (1 nm) FTS monolayers.

Experiments [57] performed with polysilicon micromotors lubricated with various dichloro- and trichlorosilane coatings have shown that the best performance was obtained with OTS coating. The OTS-lubricated micromotors exhibited relatively stable rotor speed, minimum operating voltage, and a reduction in the flange frictional force-to-torque ratio by a factor of about 1.5, even after extended storage in room air.

The hydrocarbon (HC) long-chain silane molecules grafted onto hydrated SiO_2/Si macro heterostructures have shown good tribological behavior [51,52]. The SiO_2 surface was cleaned by a xylene treatment at 250°C for 20 min. After rinsing in pure water, the sample was dipped into a sulphochromic solution or ammonia hydrogen peroxide mixture, for 15 min and rinsed with flowing pure water. The hydroxylated SiO_2 sample was then dried at 140°C in vacuum (0.2 Pa) for 2 h; the condensation reaction on the Si/SiO_2 wafer was

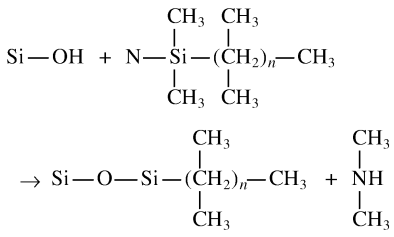

where $n = 17$ or 21. The reaction was performed in a reactor in a nitrogen flow at 180°C for 48 h, following a cleaning procedure and a dehydration process under vacuum (0.4 Pa). Grafting reagents have been synthesized. Monofunctional silanes and mainly dimethyl aminosilane were chosen as they lead to high coverage rates.

The lubrication of MEMS polysilicon microstructures by alkylsiloxane and fluoralkylsiloxane self-assembled monolayers was very effective [53]. The coefficient of static friction was found to decrease from 2.3 for an SiO_2 coating to 0.13 and 0.10 for the octadecyltrichlorosilane (OTS) and 1H,1H,2H,2H-perfluorodecyltrichlorosilane (FDTS) SAM films, respectively.

Novel composite polymeric material thin films can be formed by a combination of self-assembling chemisorption and physical adsorption of organic molecules/polymers with different substrates [54]. With such an approach, the first stage consists of surface modification with appropriate chemical functionality (e.g. NH_2 and OH terminal groups) via chemical self-assembly. The second stage involves selective adsorption of various polymer "building blocks" and their tethering to the functionalized surface through specific interactions (e.g. Coulombic, covalent, or hydrogen binding). The compounds shown below in Fig. 3 which formed molecular layers (0.4–1 nm thick) composed of SAM with functional terminal groups coated by molecular polymer layers have shown good tribological properties [54]. The substrates were silicon wafers of the (1 0 0) orientation and polysilicon surfaces of microvibromotors. Low friction coefficients (to 0.05–0.1) along with much reduced adhesion and good wear stability were observed. The best performance was found in the case of NH_2/PTA1 composition (see Fig. 3).

The use of ultrathin, hydrophobic films to reduce adhesion and stiction in MEMS has been demonstrated in recent studies [58–62, 67–72]. The integration of the OTS monolayer treatment into post-release rinse processing greatly reduces the tendency for microstructure stiction during rinsing and drying

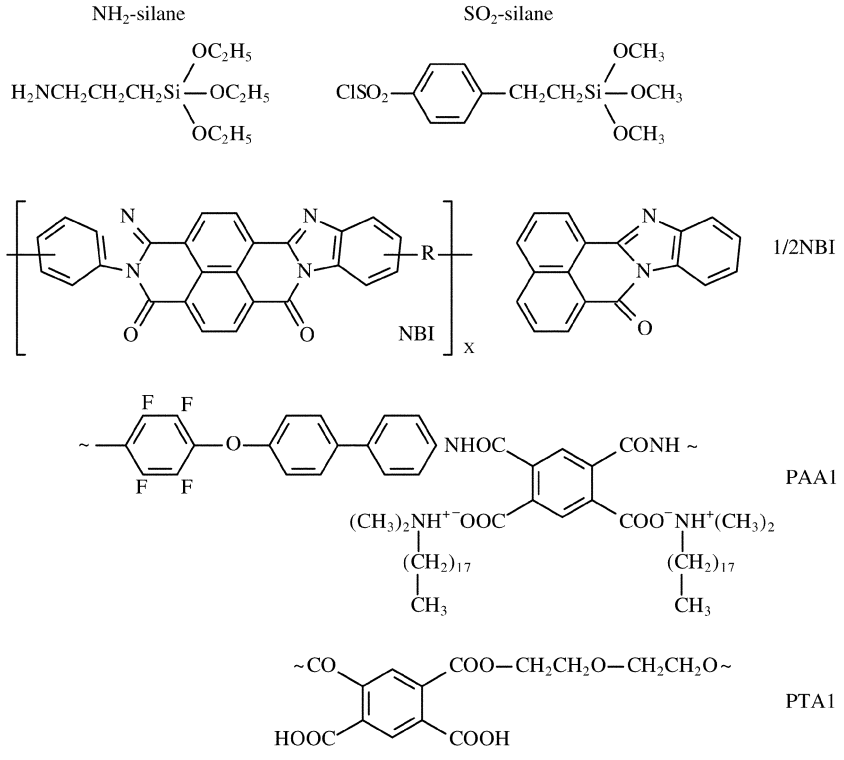

Fig. 3. Chemical formulas of some compounds used for MEMS lubrication in studies [54].

[58]. This may be atributed to the weak van der Waals and capillary forces produced due to the low surface energy (20.6 mJ/m^2) and large water contact angle (about 111° of OTS monolayers [2, 56]. Another hydrophobic coating explored was based on silicon–hydrogen bonds using ammonium fluoride treatment [59]. Hydrophobic coating formed by plasma polymerization of fluorocarbon (FC) films such as trifluoromethane has also been investigated [60,70]. The deposition of a relatively conformal, 10–20-nm-thick FC coating formed by plasma polymerization of decafluorobutane (C_4F_{10}) on a field-free zone to eliminate in-use stiction was also effective [61]. Using this method, FC-coated polysilicon cantilevers 10–194 μm long and 2 μm thick, with a gap height of 1.5 μm remained free even after direct immersion in water. Initial accelerated aging tests indicated that the film withstands temperatures up to 400°C . Wear tests showed the film remains effective after 10 million contact cycles. It is expected that Teflon (PTFE)-like plasma polymerized films will eliminate adhesion and friction in MEMS [62, 71].

A plausible model for the adsorption and subsequent binding of silane precursors to silicon surfaces is shown in Fig. 4 [2]. When precursor molecules contact the OH-terminated substrate surface having a physisorbed water monolayer, the $SiCl_3$ bonds hydrolize (Fig. 4a). Subsequently, the OH groups of the SAM precursor and water monolayer condense to form Si–O–Si siloxane linkages (Fig. 4b), whereas the remaining Si–OH bonds on the silane molecules condense to form more siloxane bonds. Finally, the resulting monolayer is covalently bonded both to itself (cross linkage) and the substrate surface (grafting) (Fig. 4c). Thus, the chemical state of exposed silicon and silicon oxide surfaces can be modified by the adsorption of SAM films possessing different functional head groups such as alkyl chains (CH_3), ester, and vinyl groups.

Concept of self-lubrication

Another possibility of decreasing stiction, friction and wear in MEMS is self-lubrication. For such purposes ultrathin films (below 300 nm thick) can be applied if the lubricants incorporated into the film's material. In our laboratory we test ultrathin films of silicon dioxide and silicon nitride, i.e. the materials compatible with the IC silicon technology. Such films produced in the laboratory of the Department of Chemistry of our university contain organic substances playing the role of lubricant during friction process.

For the manufacture of the films a special, very cheap and simple technique of glow discharges stabilized by a dielectric barrier is applied [63]. The glow discharges are of a non-uniform character and are similar to the silent discharges. The films are produced at atmospheric pressure and at relatively low temperature (below 300°C). These ultrathin films (below 300 nm thick) consisting mainly of silicon dioxide or silicon nitride are produced by polycondensation of tetraethoxysilane (TEOS) or hexamethylodisilazane (HMDSN)

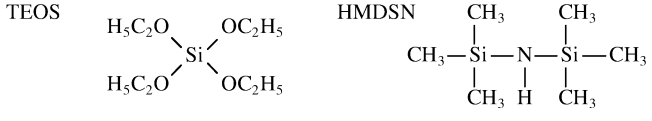

vapours, respectively, in mixtures with argon, oxygen, nitrogen or ammonia. The films are manufactured using a reactor with two parallel electrodes separated by a discharge gap of 1–3 mm width. The discharges are stabilized by a dielectric barrier 1 mm thick made of glass or quartz plate placed directly on the electrode or are manufactured in the form of an organic polymer (e.g. PET foil) 0.1–0.2 mm thick. The reactor and

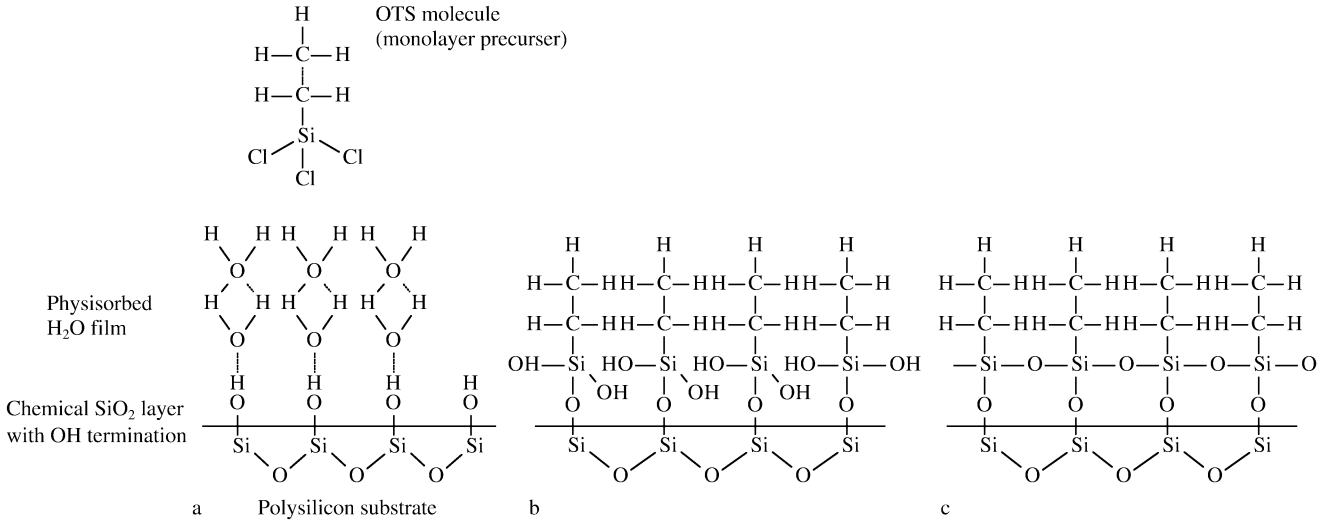

Fig. 4. Proposed mechanism of OTS self-assembled monolayer formation. **a** Liquid-phase application and hydrolisis, **b** molecule adsorption through the formation of Si–O–Si siloxane bonds, and **c** cross-linkage through covalent bonding between molecules [2]

set-up used for deposition of the films are described elsewhere [63–65].

The substrate used for the deposition of the films was p-type undoped single-crystal silicon (1 0 0) wafer. The films were amorphous. The control of deposition conditions are very important. Changing the deposition conditions leads to the change in composition of the film, i.e. it may be very soft containing organic substances and also it can be very hard with low percentage of organic substances as compared to the base material (silicon dioxide or silicon nitride). The composition of the films were studied using FTIR and XPS techniques to identify their chemical composition. For relatively soft films of silicon dioxide the amount of silicon can be about 25% (about 70% of oxygen and 4% of carbon) while for the relatively hard film the percentage of silicon can reach 65% (12% of oxygen, 23% of carbon).

The hard films exhibit very good mechanical and wear properties [64, 65]. The nanomechanical studies (using Hysitron Triboscope [66]) of the hardness and elasticity modulus of the films below 300 nm thick have shown that very soft films of silicon dioxide demonstrate hardness about 4–5 GPa while the relatively hard film can exhibit hardness about 18 GPa. Harder films demonstrated higher wear resistance. Atomic Force Microscopy (AFM) studies revealed that the surfaces of the investigated films were relatively smooth (in the range of nanoroughness). Some samples exhibited sharp nanohills demonstrating the possibility of applying such rough films as potential anti-stiction coatings in MEMS.

The self-lubricating ultrathin films of silicon dioxide or silicon nitride containing organic substances playing the role of chemically incorporated lubricant seems to be very effective solutions of stiction, friction and wear problems in MEMS.

The manufacturing technique and nanomechanical behaviour of such ultrathin films are discussed in details in Part 2 of the paper.

Summary

Stiction, friction and wear are very important problems which must be solved in the near future for production of reliable and long lasting MEMS. The lubrication with ultrathin films or organic substances is one of the ways to solve these problems. The modification of surface chemical properties (e.g. wetting and surface energy) by various surface passivation treatments, deposition of hydrophobic coatings, and lubrication with low surface energy self-assembled monolayers are effective methods for enhancing the fabrication and tribological performance of MEMS.

Another possibilty is the use of self-lubricating ultrathin films containing organic substances playing the role of chemically incorporated lubricant. Surface engineering e.g. formation of standoff bumps and microscale texturing is also an interesting way to decrease in particular in-use stiction of microstructures in MEMS.

References

1. **Maddou M** (1997) Fundamentals of Microfabrication. CRC Press, Boca Raton
2. **Komvopoulos K (1996)** Wear 200: 305–327
3. **Mehregany M; Senturia SD; Lang JH (1992)** IEEE Trans Electron Devices 39: 1136–1143
4. **Rymuza Z** (1993) Pomiary Automatyka Kontrola 9: 215–219, (in Polish)
5. **Mastrangelo CH; Hsu CH** (1993) Microelectromech Systems 2: 33–55
6. **Legtenberg R; Tilmans HAC; Elders J; Elwenspoek M** (1994) Sensors and Actuators A43: 230–238
7. **Abe T; Messner WC; Reed ML** (1995) J Microelectromech Systems 4: 66–74
8. **Mehregany M; Senturia SD; Lang JH; Nagarkar P** (1992) IEEE Trans Electron Devices 39: 2060–2069
9. **Deng K; Mehregany M; Dewa AS** (1994) J Microelectromech Systems 3: 126–133
10. **Frangoul AG; Sundram KB** (1995) J Micromech Microeng 5: 11–17
11. **Fan LS; Woodman SJ; Crawforth L** (1995) Sensors and Actuators A48: 221–227

12. **Garcia EJ; Sniegowski JJ** (1995) 1995 Sensors and Actuators A48: 203–214
13. **Mehregany M; Bart SF; Tavrow LS; Lang JH; Senturia SD; Schlecht MF** (1990) Sensors and Actuators A21–23: 173–179
14. **Tai YC; Muller RS** (1989) Sensors and Actuators 20: 49–55
15. **Wallrabe U; Bley P; Krevet B; Menz W; Mohr J** (1994) J Micromech Microeng 4: 40–45
16. **Hirano T; Furuhata T; Fujita H** (1995) IEICE Trans Electron E78–C: 132–138
17. **Dhuler VR; Mehregany M; Phillips SM** (1993) IEEE Trans Electron Devices 40: 1985–1989
18. **Huang JB; Mao PS; Tang QY; Zhang RQ** (1993) Sensors and Actuators A35: 171–174
19. **Huang JB; Tong QY; Mao PS** (1992) Sensors and Actuators A35: 69–75
20. **Wallrabe U** (1992) Dissertation, Universitat Karlsruhe
21. **Rymuza Z** (1989) Tribology of Miniature Systems. Elsevier Science Publishers, Amsterdam
22. **Tavrow LS; Bart SF; Lang JH** (1992) Sensors and Actuators A35: 33–34
23. **Phillips SM; Mehregany M** (1993) Sensors and Actuators A36: 249–254
24. **Bart SF; Mehregany M; Tavrow LS; Lang JH; Senturia SD** (1992) IEEE Trans Electron Devices 39: 566–575
25. **Mehregany M; Tai YC** (1991) J Micromech Microeng 1: 73–85
26. **Guckel H; Christensen T; Skrobis** (1992) J Micromech Microeng 2: 225–228
27. **Fujita H** (1995) Microsystem Technol 1: 93–97
28. **Bhushan B; Venkatesan S** (1993) Adv Inform Storage Systems 5: 211–239
29. **Deng K; Ko WH** (1993) Sensors Actuators A35: 45–50
30. **Gupta BK; Chevalier J; Bhushan B** (1993) Trans ASME – Tribol 112: 392–399
31. **Miyamoto T; Miyake S; Kaneko R** (1993) Wear 162–164: 733–738
32. **Deng K; Ko WH** (1992) J Micromech Microeng 2: 14–20
33. **Suzuki S; Matsuura T; Uchizawa M; Yura S; Shibata H** (1991) Proc IEEE Micro Electro Mechanical System Workshop, Nara, February, Japan, pp 143–147
34. **Noguchi K; Suzuki M; Fujita H; Yoshimura N** (1991) Trans IEE Japan 11-D: 592–593, in Japanese
35. **Beerschwinger U; Albrecht T; Mathieson D; Reuben RL; Yang SJ; Taghizadeh M** (1995) Wear 181–183: 426–435
36. **Beerschwinger U; Yang SJ; Reuben RL; et al** (1994) J Micromech Microeng 4: 14–22
37. **Beerschwinger U; Mathieson D; Reuben RL; Yang SJ** (1994) J Micromech Microeng 4: 95–105
38. **Beerschwinger U** (1995) PhD Thesis, Heriot-Watt University, Edinburg (GB)
39. **Bayer RG** (1982) Wear 69: (1982) 235–239
40. **Ohmae N** (1995) Proc 1st Int Micromachine Symp November 1–2, Tokyo, Japan, Micromachine Center, pp 47–53
41. **Mizuhara K; Hsu SM** Proc 19th Leeds-Lyon Symp on Wear Particles. Dowson D; Taylor CM; Godet M eds, Elsevier, Amsterdam, pp 323–328
42. **Mehregany M; Dhuler VR** (1992) J Micromech Microeng 2: 1–3
43. **Deng K; Ramanathan GP; Mehregany M** (1994) J Micromech Microeng 4: 266–269
44. **Zhang X; Tang WC** (1995) Sensors and Materials 7: 415–430
45. **Cho YH; Pisano AP; Howe RT** (1994) J Microelectromech Systems 3: 81–87
46. **Cho YH; Kwak BM; Pisano AP; Howe RT** (1994) Sensors and Actuators A44: 31–39
47. **Watanabe S; Suzuki M; Yoshimura N; Fujita H** (1994) Trans IEE Japan 114–A: 168–172 (in Japanese)
48. **Busch-Vishniac IJ** (1992) Sensors and Actuators A33: 207–220
49. **Omar MP; Mehregany M; Mullen RL** (1992) J Microelectromech Systems, 1: 130–139
50. **Lim DS; Danyluk S** (1998) J Mater Sci 23: 2607–2612
51. **Clechet P; Martelet C; Belin M; Zarrad H; Jaffrezic-Renault N; Fayeulle S** (1994) Sensors and Actuators A44: 77–81
52. **Zarrad H; Clechet P; Belin M; Martelet C; Jaffrezic-Renault N** (1995) Tribol Int 28: 241–243
53. **Srinivasan U; Howe RT; Maboudian R** (1998) Tribology Issues and Opportunities in MEMS, Bhushan B ed, Kluwer Academic Publishers, Dordrecht, pp 597–606
54. **Tsukruk VV; Nguyen T; Lemieux M; Hazel J; Weber WH; Shevchenko VV** (1998) **Klimenko N; Sheludko E** Tribology Issues and Opportunities in MEMS, Bhushan B ed, Kluwer Academic Publishers, Dordrecht, 607–614
55. **Pomerantz A; Segmuller A; Netzer L; Sagiv J** (1985) Thin Solid Films, 132: 153–162
56. **DePalma V; Tillman N** (1989) Langmuir 5: 868–872
57. **Deng K; Collins RJ; Mehregany M; Sukenik CN** (1995) Proc IEEE Micro Electro Mechanical Systems, Amsterdam, Netherlands, 29 January–2 February 1995, pp 368–373
58. **Fujita H** (1995) Microsystem Technol 1: 93–97
59. **Houston MR et al** (1995) Transducers'95, pp 210–213
60. **Jansen HV et al.** (1994) Sensors Actuators, A41–42: (1994) 136–140
61. **Man PF; Gogoi BP; Mastrangelo H** (1997) J Microelectromech Systems 6: 25–34
62. **Matsumoto Y** (1998) Micromachine May 23: 8
63. **Schmidt-Szałowski K; Fabianowski W; Rżanek-Boroch Z; Gutkowski M** (1996) Proc Int Symp on high Pressure low temperature Plasma chemistry „HAKONE 5", Contributed Papers, Milovy, Czech Republik, September 2–4, pp 190–194
64. **Rymuza Z; Kusznierewicz Z; Misiak M; Schmidt-Szałowski K; Rżanek-Boroch Z; Sentek J** (1998) Tribology Issues and Opportunities in MEMS, Bhushan B ed, Kluwer Academic Publishers, Dordrecht, pp 579–589
65. **Rymuza Z; Piątkowska A; Kusznierewicz Z; Misiak M; Jagielski J; Schmidt-Szałowski K; Rżanek-Boroch Z** (1998) Proc Industrial and Automotive Lubrication, 11th Int Colloquium 13–15 January 1998, Bartz WJ ed, Technische Akademie Esslingen, Vol III, 2077–2082
66. **Bhushan B; Kulkarni A; Bonin W; Wyrobek J** (1996) Philo Mag A74: 1117–1128
67. **Maboudian R; Howe RT** (1997) J Vacuum Sci Technol B 15: 1–20
68. **Maboudian R; Howe RT** (1997) Tribol Lett 3: 215–221
69. **Henck SA** (1997) Tribol Lett 3: 239–247
70. **Mastrangelo CH** (1997) Tribol Lett 3: 223–238
71. **Smith BK; Sniegowski JJ; LaVigne G; Brown C** (1998) Sensors and Actuators A70: 159–163
72. **Srinivasan U; Houston MR; Howe RT** (1998) J Microelectromech Systems 7: 252–259